

# CNG engines exhaust gas treatment via Pd-Spinel-type-oxide catalysts

D. Fino<sup>\*</sup>, N. Russo, G. Saracco, V. Specchia

*Department of Materials Science and Chemical Engineering, Politecnico di Torino, Corso Duca degli Abruzzi 24, 10129 Torino, Italy*

Available online 13 July 2006

## Abstract

Four spinel-type catalysts  $AB_2O_4$  ( $CoCr_2O_4$ ,  $MnCr_2O_4$ ,  $MgFe_2O_4$  and  $CoFe_2O_4$ ) were prepared and characterized by XRD, BET, TEM and FESEM techniques. The activity of these catalysts towards the combustion of methane was evaluated in a temperature-programmed combustion (TPC) apparatus. Spinel-type-oxides containing Cr at the B site were found to provide the best results. The half-conversion temperature of methane over the  $CoCr_2O_4$  catalyst was 376 °C with a  $W/F = 0.12 \text{ g s/cm}^{-3}$ . On the basis of temperature-programmed oxygen desorption (TPD) analysis as well as of catalytic combustion runs, the prevalent activity of the  $CoCr_2O_4$  catalyst could be explained by its higher capability to deliver suprafacial, weakly chemisorbed oxygen species. This catalyst, promoted by the presence of 1 wt% of palladium deposited by wet impregnation, was lined on cordierite monoliths and then tested in a lab-scale test rig. The combination of Pd and  $CoCr_2O_4$  catalysts enables half methane conversion at 330 °C (GHSV =  $10,000 \text{ h}^{-1}$ ), a performance similar to that of conventional 4 wt% Pd- $\gamma\text{-Al}_2\text{O}_3$  catalysts but enabled with just a four-fold lower amount of noble metal.

© 2006 Elsevier B.V. All rights reserved.

**Keywords:** CNG engines; Methane catalytic combustion; Spinel-type-oxide;  $\gamma$ -Alumina

## 1. Introduction

Advanced natural gas engines guarantee considerable advantages over conventional gasoline and diesel engines. Natural gas (NG) is a largely available form of fossil energy and therefore non-renewable. However, NG has some advantages compared to gasoline and diesel from an environmental perspective. Natural gas is composed primarily of methane ( $\text{CH}_4$ ) but includes other HC compounds in small amounts (e.g. propane, butanes and pentanes). It is a cleaner fuel than either gasoline or diesel as far as emissions are concerned. NG has a high octane number (RON = 110–130) and therefore can be easily employed in spark-ignited internal combustion engines. It has also a wider flammability range than gasoline and diesel oil. However, the engine power density is reduced with  $\text{CH}_4$  because the volume of the gas reduces the air intake capacity of the engine. The low flame temperature of lean-operated CNG engines helps to limit the formation of  $\text{NO}_x$ . Furthermore, since NG contains only 75 wt% carbon versus 86–88 wt% of gasoline or diesel, it produces less  $\text{CO}_2$  per unit of energy released. Other

benefits lie in the fact that NG is neither toxic or carcinogenic, nor caustic. CNG is likely to be safer than gasoline or diesel, owing to its low density, high ignition temperature (540 °C) and high flammability limits which play in favour of a comparatively fast dispersion of  $\text{CH}_4$  losses and render it less likely to ignite [1].

As underlined above, from the environment impact viewpoint, CNG engines could lead to very low pollutant emissions. However, unburned methane is harder to oxidise than gasoline-derived unconverted HC's. The strong greenhouse effect of methane (more than one order of magnitude higher than that of  $\text{CO}_2$ ) induces increasing concern at a legislation level and the development of a new after treatment technologies [2–4]. Catalytic combustion of methane on honeycomb converters similar to those used for the treatment of gasoline engine exhaust gases is the way to go.

Particular requirements are imposed on the catalysts for methane combustion. They must resist thermal and mechanical shocks and exhibit high activity, which is not trivial owing to the high stability of  $\text{CH}_4$  and the low temperature of the exhausts of CNG vehicles (hardly exceeding 500 °C). Commercial catalysts are mostly based on  $\gamma\text{-Al}_2\text{O}_3$ -supported Pd [5–8], having at least a three-fold higher noble metal loading compared to that of conventional three-way catalysts. A research line carried out at Politecnico di Torino in

<sup>\*</sup> Corresponding author. Tel.: +39 011 5644710; fax: +39 011 5644699.

E-mail address: [debora.fino@polito.it](mailto:debora.fino@polito.it) (D. Fino).

cooperation with the FIAT Research Centre (Orbassano, Italy), is aimed at developing nanostructured Pd-spinel-type-oxide catalysts employing an overall noble metal load markedly smaller than that used in conventional converters. The present manuscript concerns the development of these catalysts. The performance of the most promising developed catalyst, once deposited on a honeycomb catalytic converter and tested in a lab-scale test rig, is also presented and discussed.

## 2. Experimental

### 2.1. Catalyst preparation and characterization

A series of spinel catalysts ( $\text{CoCr}_2\text{O}_4$ ,  $\text{MnCr}_2\text{O}_4$ ,  $\text{MgFe}_2\text{O}_4$  and  $\text{CoFe}_2\text{O}_4$ ) were prepared via a highly exothermic and self-sustaining reaction, the so-called “solution combustion synthesis” (SCS) method [9]. This technique is particularly suitable for production of nanosized particles. A concentrated aqueous solution of various precursors (metal nitrates and urea) was located in an oven at  $600\text{ }^\circ\text{C}$  for few minutes in a crucible, so as to ignite the very fast synthesis reactions. The adoption of the SCS method entails the formation of pure oxide catalysts with rather high specific surface areas in the absence of any carrier. This allows to better compare the intrinsic catalytic activity of the series of prepared compounds.

On the  $\text{CoCr}_2\text{O}_4$  catalyst, owing to its superior performance, Pd was then deposited by wet impregnation with an aqueous solution of  $\text{Pd}(\text{NO}_3)_2$  so as to obtain 6 wt% of Pd. This latter catalyst was then kept at  $500\text{ }^\circ\text{C}$  in air in order to promote Pd stabilization and the formation of finely dispersed Pd/PdO clusters. A calcination step at  $700\text{ }^\circ\text{C}$  for 2 h was finally performed. All the catalysts were then ground in a ball mill and characterized by different analyses (XRD-PW1710 Philips diffractometer equipped with a monochromator for the  $\text{Cu K}\alpha$  radiation, BET–Micromeritics ASAP 2010, FESEM-Leo 50/50 VP with Gemini column, TEM-Philips CM 30 T) in order to check the achievement of the desired microstructure and chemical composition. The activities of the prepared catalysts were analyzed by temperature-programmed combustion (TPC), according to the following standard screening operating procedures: a gas mixture (2.5 vol%  $\text{CH}_4$ ; 7.5 vol%  $\text{O}_2$ , He balance) was fed at the constant rate of  $0.83\text{ ml s}^{-1}$  to a fixed-bed micro reactor constituted of 100 mg of catalyst and 900 mg of  $\text{SiO}_2$  ( $W/F = 0.12\text{ g s/cm}^{-3}$ ). Starting from  $750\text{ }^\circ\text{C}$ , the inlet temperature, measured by a K-type thermocouple placed alongside the quartz tube, was decreased at a  $2\text{ }^\circ\text{C min}^{-1}$  rate and the outlet  $\text{CO}_2$ ,  $\text{CO}$ ,  $\text{CH}_4$  and  $\text{O}_2$  concentrations were determined by continuous NDIR and paramagnetic analyzers (ABB), thus allowing the authors to calculate methane conversion and close the carbon balances (relative error,  $\pm 4\%$ ). The activity of the prepared catalysts was also analyzed with a 0.4%  $\text{CH}_4$  inlet, more representative of real exhaust gas composition.

From the obtained typical sigma-shaped curves, methane half-conversion temperatures ( $T_{50}$ ) were evaluated as an index of catalytic activity towards methane combustion. Each data point was obtained as the average of three twin runs performed

on different samples of the same catalytic material. The deviation between the conversion measured at the same temperature in such runs was always within  $\pm 15\text{ }^\circ\text{C}$ . In order to fully appreciate the catalytic effect of the spinels, blank runs in the absence of the catalyst and in the presence of just  $\text{SiO}_2$  were also carried out.

Some further analyses were performed on the prepared spinel catalysts in a temperature-programmed desorption/reduction/oxidation (TPD/R/O) analyser, equipped with a thermal conductivity (TCD) detector (TPD/R/O 1100 Thermoquest). A fixed bed of catalyst was enclosed in a quartz tube and sandwiched between two quartz wool layers; before each temperature-programmed desorption run, the catalyst was heated under an  $\text{O}_2$  flow (40 N ml/min) up to  $750\text{ }^\circ\text{C}$ . After 30 min at this temperature as a common pretreatment, the reactor temperature was then lowered to room temperature with the same flow rate of oxygen, thereby allowing complete oxygen adsorption over the catalyst. Afterward, helium was fed to the reactor at a rate of 10 ml/min, which was kept for 1 h at room temperature to purge any excess oxygen molecules. The catalyst was then heated to  $1100\text{ }^\circ\text{C}$  at a constant rate of  $10\text{ }^\circ\text{C/min}$  under a helium flow rate of 10 N ml/min.

A detailed description of oxygen TPD analysis was reported in ref. [10]. X-ray diffraction was once again performed on the catalysts which underwent TPD analysis, to check whether the spinel structure had been retained or not, and to check for the possible appearance of new phases.

### 2.2. Catalytic monolith preparation and characterization

The catalytic converters (cylindrical cordierite honeycombs by Chauger; cell density = 200 cpsi; length = 25 mm; diameter = 34 mm) were prepared by a preliminary deposition of a layer of  $\gamma$ -alumina by in situ SCS [11] (10 wt% referred to the monolith weight) and then 15 wt% (referred to the  $\gamma$ -alumina weight) of  $\text{CoCr}_2\text{O}_4$ , the most active spinel catalyst. Pd was then deposited by wet impregnation with an aqueous solution of  $\text{Pd}(\text{NO}_3)_2$  so as to obtain 1 wt% of Pd referred to the  $\gamma$ -alumina (about  $80\text{ g/ft}^3$  of catalytic converter). The relative amount of Pd versus the  $\text{CoCr}_2\text{O}_4$  is nearly equivalent to the bulk, unsupported 6 wt% Pd- $\text{CoCr}_2\text{O}_4$  prepared in powder form. These monoliths were then kept at  $500\text{ }^\circ\text{C}$  in air in order to promote the Pd stabilization and the formation of finely dispersed Pd/PdO clusters. A calcination step at  $700\text{ }^\circ\text{C}$  for 2 h was finally performed.

Adhesion tests and structural characterization (XRD, FESEM and TEM) were carried out. The adhesion properties between the catalyst and ceramic surface were checked by means of ultrasonic bath test: a piece of the catalytic monolith was weighted before and after a standard ultrasonic treatment [12] to quantify the catalyst loss.

Physicochemical characterization was performed on sections of the catalytic monolith; in particular, scanning electron microscopy (SEM) analyses were performed using a Philips 515 SEM apparatus equipped with an energy-dispersive spectrometer (EDAX 9900 EDS), in order to investigate the morphology and composition of the deposited catalytic layer.

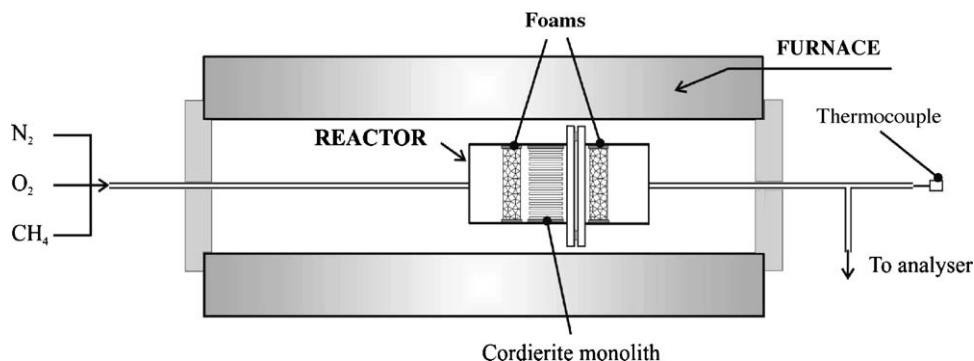


Fig. 1. Scheme of experimental set-up.

Catalytic combustion experiments were performed in a stainless steel reactor (Fig. 1) heated in a horizontal split tube furnace with a heating length of 60 cm. The catalyzed monolith was sandwiched between two mullite foams to optimize flow distribution. For the temperature control, a thermocouple, inserted along one of the central monolith channel, was used to measure the inlet temperature. Lean inlet conditions (0.4 vol% CH<sub>4</sub>, 10 vol% O<sub>2</sub>, N<sub>2</sub> balance) were ensured via mass flow controllers. The reactor temperature gradient measured in the axial direction was not significant. The GHSV was set equal to 10,000 h<sup>-1</sup>, whereas the composition of the off-gases was monitored by the same equipment described above.

A converter containing 4 wt% of Pd- $\gamma$ -alumina, simulating a commercial catalyst was also prepared by impregnation of a bare  $\gamma$ -alumina coated monolith and tested under the above reference conditions.

### 3. Results and discussion

The XRD spectra (not reported) of the prepared spinel catalysts showed diffraction peaks corresponding to the desired catalysts structure; no diffraction peaks related to other phases were detected. Fig. 2 shows a TEM micrograph of the CoCr<sub>2</sub>O<sub>4</sub> spinel-type catalyst. It refers to the catalyst that showed the highest surface area and activity among those prepared. No indications of the possible presence of amorphous or minor crystalline phases is perceivable in Fig. 2 or in any TEM observation made on the other three Pd-free catalysts. Most of the spinel crystals range between 20 and 50 nm in size, which is in accordance to the B.E.T. specific surface areas measured (10–60 m<sup>2</sup>/g, see Table 1). Moreover, Table 1 lists, beyond the B.E.T. values, the methane half-conversion temperatures of the fresh spinel-type catalysts with two different inlet conditions and Fig. 3 shows the methane conversion versus temperature plots as recorded with the catalysts considered, also containing the 6 wt% of Pd. All catalysts guarantee much lower  $T_{50}$  values than the one related to non-catalytic combustion (816 °C). The CoCr<sub>2</sub>O<sub>4</sub> + 6 wt% Pd catalyst gave the best performance with a  $T_{50}$  value of 370 °C.

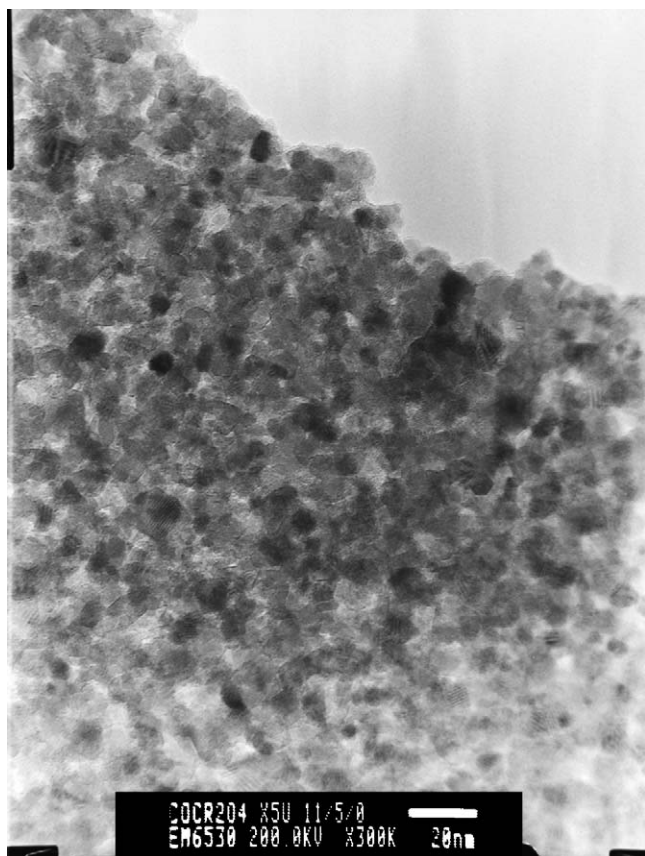
Fig. 2. TEM micrograph of the CoCr<sub>2</sub>O<sub>4</sub> spinel-type catalyst.

Table 1

Results of the screening tests on the activity:  $T_{50}$ , methane half-conversion temperature and B.E.T. specific surface area of various spinel catalysts developed at different feed gas mixtures (CH<sub>4</sub>/O<sub>2</sub>, He balance)

Catalysts	B.E.T. [m <sup>2</sup> /g]	$T_{50}$ [°C], 2.5% CH <sub>4</sub> –7.5% O <sub>2</sub>	$T_{50}$ [°C], 0.4% CH <sub>4</sub> –10.0% O <sub>2</sub>
6 wt% Pd on CoCr <sub>2</sub> O <sub>4</sub>	60	370	321
CoCr <sub>2</sub> O <sub>4</sub>	59	375	327
MnCr <sub>2</sub> O <sub>4</sub>	37	380	330
CoFe <sub>2</sub> O <sub>4</sub>	10	549	498
MgFe <sub>2</sub> O <sub>4</sub>	34	580	532
Blank-without catalyst	–	816	761

The value concerning the non-catalytic methane combustion is shown for a comparison.

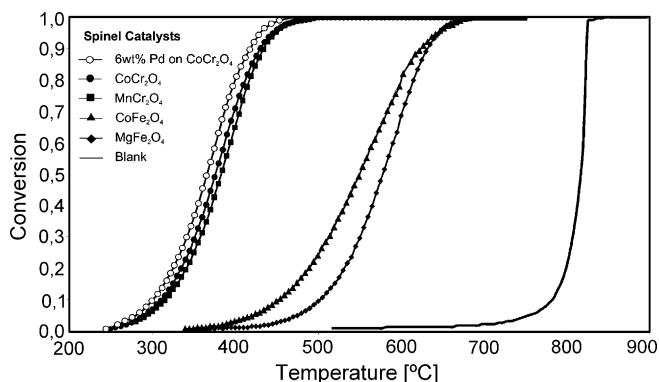


Fig. 3. Methane conversion vs. temperature plots: comparison of the catalysts considered with the non-catalytic blank.

The SCS technique was adopted to obtain extremely pure spinels with a good specific surface area despite the absence of any carrier. This allowed a deeper investigation of the mechanistic aspects of the  $\text{CH}_4$  catalytic combustion over the active phase alone with no interference or synergetic effects of the carrier. The latter was adopted in the catalytic monoliths preparation to maximise the specific amount of active sites.

As noted above a transient TPD study was carried out to better clarify the rationale of the different catalytic activities. In particular, Fig. 4 shows the results obtained during oxygen TPD runs that were quite helpful in elucidating the behavior of catalysts towards methane combustion. As thoroughly discussed in a previous paper of ours [11], perovskites can desorb two different types of oxygen species as the temperature is increased: a low temperature specie, named  $\alpha$  or suprafacial, desorbed in the 300–600 °C range, and a high temperature one, named  $\beta$  or intrafacial, desorbed above about 600 °C. The same behavior was observed for spinels. If attention is focused on the temperature range below 600 °C (inside the  $\alpha$  oxygen region), where the most active spinels tested displayed their best methane combustion activities (see the conversion curves in Fig. 3), oxygen desorption capability is in line with the activity order ( $\text{CoCr}_2\text{O}_4 > \text{MnCr}_2\text{O}_4 > \text{CoFe}_2\text{O}_4 > \text{MgFe}_2\text{O}_4$ ). The temperature at which  $\alpha$  oxygen is desorbed and the amount of desorbed oxygen seem to be the key factors determining the catalytic activity of pure spinels. The activity of  $\text{MnCr}_2\text{O}_4$  and  $\text{CoCr}_2\text{O}_4$  is quite similar and the correlation between activity and suprafacial oxygen is not enough evident. It has to be

Table 2

Collection of results of temperature-programmed desorption of suprafacial  $\alpha$  and  $\beta$  intrafacial oxygen as derived from the plots in Fig. 4

Catalyst	$\text{O}_2$ total [ $\mu\text{mol/g}$ ]	$\text{O}_2$ $\alpha$ 600 °C [ $\mu\text{mol/g}$ ]	$\text{O}_2$ $\beta$ 600 °C [ $\mu\text{mol/g}$ ]
$\text{MnCr}_2\text{O}_4$	404.3	55.8	348.5
$\text{CoCr}_2\text{O}_4$	124.1	20.3	103.8
$\text{CoFe}_2\text{O}_4$	70.5	7.1	63.4
$\text{MgFe}_2\text{O}_4$	7.8	2.9	4.8

considered that oxygen desorption from  $\text{CoCr}_2\text{O}_4$  starts before that of  $\text{MnCr}_2\text{O}_4$ . Moreover, the specific surface area of cobalt chromite is higher than that of manganese chromite. These last two factors may explain why, after this screening of methane combustion on spinel-type catalysts in powder, the best catalyst was found to be  $\text{CoCr}_2\text{O}_4$ , despite the  $\text{MnCr}_2\text{O}_4$  catalyst shows much higher amounts of  $\alpha$  and  $\beta$  oxygen desorbed (Table 2).

Fig. 5 shows a FESEM micrograph of  $\gamma\text{-Al}_2\text{O}_3\text{-CoCr}_2\text{O}_4$  spinel-type catalyst deposited onto the cordierite monolith channels via SCS. Its microstructure is foamy. During combustion synthesis, the decomposition–combustion of the  $\gamma\text{-Al}_2\text{O}_3$  and of the  $\text{CoCr}_2\text{O}_4$  reacting precursors generates a large amount of gaseous products in a very short period of time, which leads to a spongy catalyst morphology. This feature favours the formation of large intra layer pores for the catalyst clusters agglomerates, which reduce the mass transfer resistance of the layer itself. The adhesion between the deposited catalyst and the channel walls of the traps was excellent, as the loss of catalyst by ultrasonic treatment was lower than 1%.

The methane conversion curves plotted in Fig. 6 versus temperature over different catalysts deposited on cordierite monolith show that all  $\gamma\text{-Al}_2\text{O}_3$ -supported catalysts shift the combustion temperature range towards values significantly lower (decrease of more than 350 °C) than those typical of non-

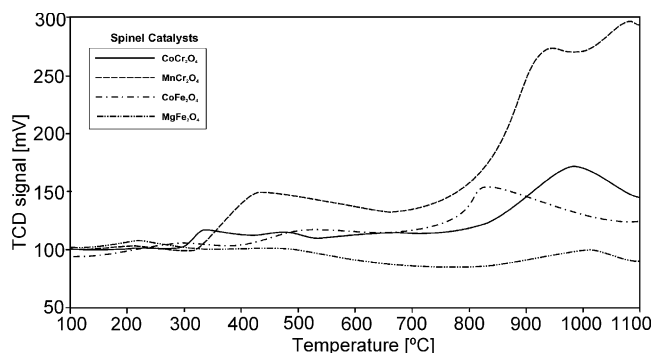


Fig. 4. Results of oxygen temperature-programmed desorption (TPD) tests on the pure spinel catalysts.

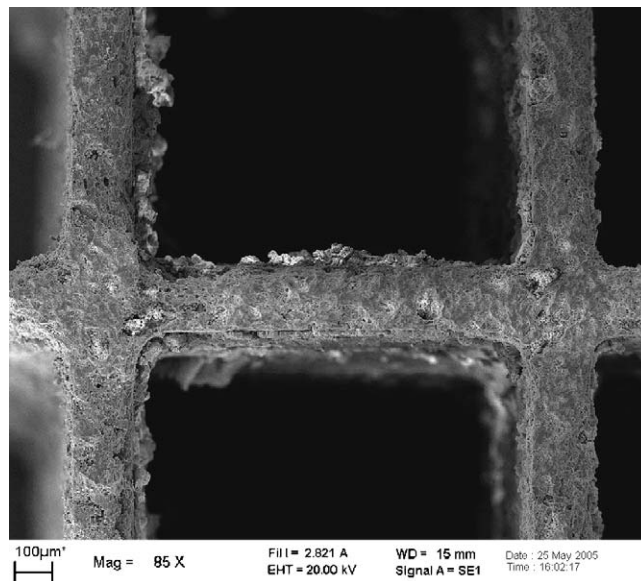


Fig. 5. FESEM micrograph of  $\text{CoCr}_2\text{O}_4$  spinel-type catalyst deposited onto the cordierite monolith channels via combustion synthesis.



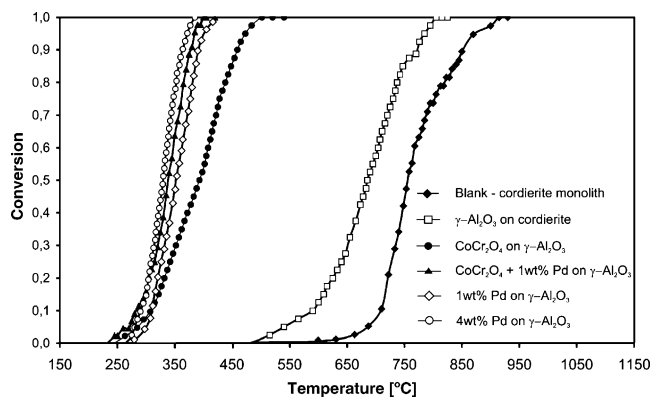


Fig. 6. Methane conversion as function of temperature over different catalysts deposited on cordierite monolith (GHSV = 10,000 h<sup>-1</sup>; feed composition = 0.4% CH<sub>4</sub>, 10% O<sub>2</sub>, N<sub>2</sub> balance).

catalytic combustion. Starting from the pure  $\gamma$ -Al<sub>2</sub>O<sub>3</sub> catalyzed monolith, only a slight improvement of the activity is noticeable compared to the blank monolith. Undoubtedly, the dispersion of active spinel-type-oxide phase (CoCr<sub>2</sub>O<sub>4</sub>) on alumina is successful to enhance the activity towards methane oxidation. The half-conversion temperature was lowered to 325 °C, from the 760 °C achieved for the uncatalyzed converter. Further lowering improvements (about 15 °C) are induced by the presence of 1 wt% of Pd, thereby approaching the performance of the high-Pd (4 wt%) containing catalysts. The different curve slope of catalysts containing Pd could be explained by the capability of Pd itself to contribute to methane ignition and combustion. It is worth noticing that the CoCr<sub>2</sub>O<sub>4</sub> + 1 wt% Pd/ $\gamma$ -Al<sub>2</sub>O<sub>3</sub> catalyst behaves slightly better than its single component counterpart (i.e., either CoCr<sub>2</sub>O<sub>4</sub> or 1 wt% Pd on  $\gamma$ -Al<sub>2</sub>O<sub>3</sub>), a likely sign of a synergism between the spinel and the Pd functionalities that still needs to be fully elucidated. Besides, the role of Pd in methane catalytic combustion is well known and still addressed by a number of investigations [6,13,14].

#### 4. Conclusions

Four spinel-type-oxide catalysts (CoCr<sub>2</sub>O<sub>4</sub>, MnCr<sub>2</sub>O<sub>4</sub>, MgFe<sub>2</sub>O<sub>4</sub> and CoFe<sub>2</sub>O<sub>4</sub>) were prepared by solution combustion synthesis, characterized and tested as catalysts for methane combustion.

As far as the comparative analysis of the activity of the catalysts towards methane combustion is concerned, specific

experiments were carried out with pure spinels in powder. After this previous activity screening, the best catalyst was found to be CoCr<sub>2</sub>O<sub>4</sub> and therefore it was selected to be deposited and tested on washcoated cordierite monolith.

Experimental tests on a series of ad hoc prepared CNG exhaust gas after treatment converters demonstrated a superior activity towards methane conversion by coupling the effects of CoCr<sub>2</sub>O<sub>4</sub> and Pd active species. This should entail a reduction of the overall catalyst costs compared to conventional Pd-only catalysts currently employed with high Pd loads. This constitutes the major driving force to spinel catalyst development in this application field. Specific activities are currently in progress either to develop more active spinel catalysts and to optimize the deposition of Pd in order to gain a further reduction of this costly noble metal in the catalyst formulation. Finally, the reader should be warned that in order to fully assess the potential of these catalysts, their performance should be checked in the presence of water vapour and after prolonged operation, which is planned for the near future.

#### References

- [1] M.L. Poulton, *Alternative Fuels for Road Vehicles*, Computational Mechanics Publications, Boston, MA, 1994.
- [2] Web site: [www.epa.gov](http://www.epa.gov).
- [3] Transportation Research Board, *Toward a sustainable future*, in: *Addressing the Long-term Effects of Motor Vehicle Transportation on Climate and Ecology*, Special Report 251, National Academy Press, Washington, DC, 1997.
- [4] Energy Information Administration, [www.eia.doe.gov/cneaf/electricity/page/primer.html](http://www.eia.doe.gov/cneaf/electricity/page/primer.html), Accessed on August 23, 2001, Electric power industry generation by energy source, Electric Power Annual 1998, vol. II, Table 1, pp. 12–13.
- [5] I. Cerri, M. Pavese, G. Saracco, V. Specchia, *Catal. Today* 83 (2003) 19.
- [6] P. Forzatti, G. Groppi, *Catal. Today* 54 (1999) 165.
- [7] D.L. Mowery, M.S. Graboski, T.R. Ohno, R.L. McCormick, *Appl. Catal., B: Environ.* 21 (1999) 157.
- [8] J.K. Lampert, M.S. Kazi, R.J. Ferrauto, *Appl. Catal., B: Environ.* 14 (1997) 211.
- [9] A. Civera, M. Pavese, G. Saracco, V. Specchia, *Catal. Today* 83 (2003) 199.
- [10] N. Russo, D. Fino, G. Saracco, V. Specchia, *J. Catal.* 229 (2005) 459.
- [11] D. Fino, N. Russo, G. Saracco, V. Specchia, *J. Catal.* 217 (2003) 367.
- [12] D. Fino, V. Specchia, *Chem. Eng. Sci.* 59 (2004) 4825.
- [13] T.V. Choudhary, S. Banerjee, V.R. Choudhary, *App. Catal., A: Gen.* 234 (2002) 1.
- [14] A. Janbey, W. Clark, E. Noordally, S. Grimes, S. Thair, *Chemosphere* 52 (2003) 1041.